Journal of Ceramic Processing Research. Vol. 15, No. 2, pp. 76~81 (2014)

JOURNAL OF
Ceramic Processing Research

Rapid sintering of nanocrystalline 2Ti-ZrO_2 composite by the pulsed current activated sintering method with high pressure at low-temperature and its characteristics

Na-Ra Park and In-Jin Shon*

Division of Advanced Materials Engineering, the Research Center of Advanced Materials Development, Chonbuk National University, 664-14 Deokjin-dong 1-ga, Deokjin-gu, Jeonju, Jeonbuk 561-756, Korea

TiO and Zr powders were used as raw materials, and were milled by high energy ball milling method and horizontal ball milling method. Highly dense nanostructured 2Ti-ZrO_2 composites were consolidated by pulsed current activated sintering method, within 4 minutes from high energy ball milled powder, and horizontal ball milled powders, under 1 GPa pressure. The relative densities of these specimens sintered from PCAS were measured by Archimedes' method. The grain sizes of ZrO_2 in the composites were calculated by Suryanarayana and Grant Norton's formula. The average hardness and fracture toughness value of nanostuctured 2Ti-ZrO_2 composite sintered from high energy ball milled powder were 1230 kg/mm^2 and 6.8 MPa · m$^{1/2}$, respectively. The wear resistance of the composite was measured by pin-on-disc type apparatus, without a lubricant. Lastly, cell viability of the composite was analyzed by absorbance, using CCK-8 solution.

Key words: Rapid sintering, Composite, Nanocrystalline, Characteristics, 2Ti-ZrO_2.

Introduction

Ceramics have been used as an alternative to metal-on-polyethylene in joint replacement surgery of arthritic hips and knees, since the 1970s [1]. The advantage of these ceramic materials in orthopedic bearings is the reduction, or possible elimination of polyethylene wear particles from the periprosthetic space [2]. Even though ceramic materials have these advantages for total joint replacement, we have to consider the low fracture toughness of ceramic materials, since the mechanical properties of materials used as the articulating surfaces in total joint replacement are important, as these materials are subjected to loads in the body. These loads vary from three times the body weight for normal walking, to eight times the body weight for jogging or stumbling [3]. Therefore, we tried to improve its fracture toughness, by adding Ti, known as having good fracture toughness and biocompatibility.

Ti has a density of 4.506 g cm^{-3}, a Young's modulus of 116 GPa, and good fracture toughness [4]. ZrO_2 has a density of 5.98 g cm^{-3}, a Young's modulus of 207 GPa, excellent oxidation resistance, and good high-temperature mechanical properties [5]. Hence, microstructure consisting of Ti and ZrO_2 may be able to satisfy the good mechanical properties requirement of successful structural material.

Nanocrystalline materials, as advanced engineering materials, have received much attention, due to their improved physical and mechanical properties. In recent research, nanocrystalline powders have been developed by co-precipitation, the thermochemical and thermomechanical process named as the spray conversion process (SCP), and high energy milling [6-8]. The grain size in sintered materials, however, becomes much larger than that in pre-sintered powders, due to fast grain growth during the conventional sintering process. Therefore, controlling the grain growth during sintering is one of the keys to the commercial success of nanostructured materials. In this regard, the pulsed current activated sintering method, which can make dense materials within 5 min, has been shown to be effective in achieving this goal [9-11].

The purpose of this work is to produce nanocrystalline 2Ti-ZrO2 composite, and to improve its mechanical properties, so as to apply it to prosthesis joint replacement. Therefore, we made nano-sized powders from the high energy ball milling method and horizontal ball milling method. The dense nanocrystalline 2Ti-ZrO_2 composites were fabricated within 4 minutes using the pulsed current activated sintering method, and we evaluated the mechanical properties (hardness, fracture toughness and wear resistance), and cell viability.

Experimental Procedure

Powders of 99.5% TiO (–325 mesh, Alfa Aesar, Inc) and 99.5% pure Zr (–325 mesh, Sejong, Inc) were used as raw materials. The TiO and Zr powders have rectangular and irregular shape, respectively, as shown in Fig. 1. TiO and Zr powders were mixed by the two types of methods, to make fine powders. Firstly, the

*Corresponding author:
Tel : +82-63-270-2381
Fax: +82-63-270-2386
E-mail: ijshon@chonbuk.ac.kr

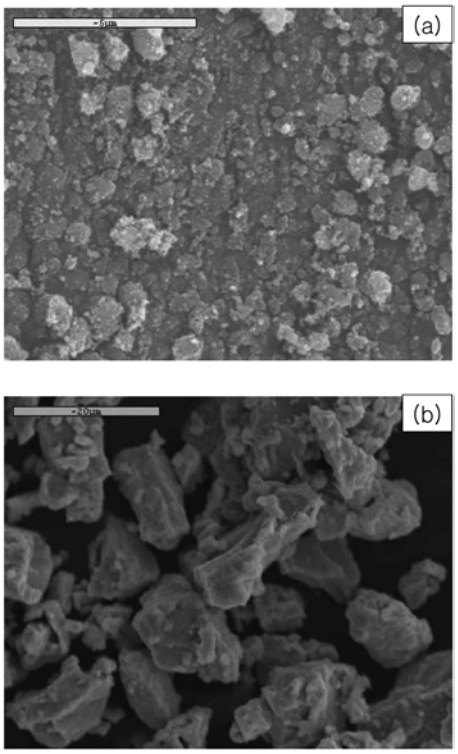

Fig. 1. Scanning electron microscope image of raw materials: (a) TiO, (b) Zr.

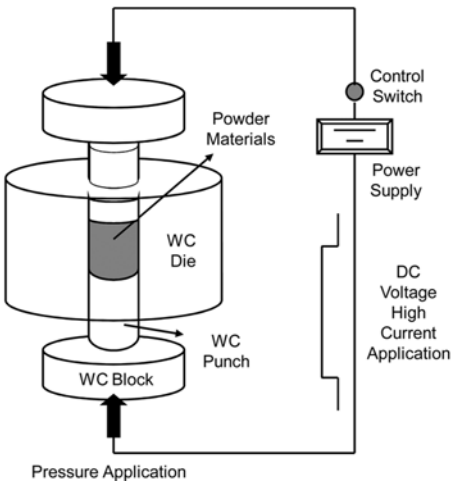

Fig. 2. Schematic diagram of the pulsed current activated sintering apparatus.

raw powders were milled by the high-energy ball milling method, Pulverisette-5 planetary mill at 250 rpm and for 10 h. Tungsten carbide balls (8.5 mm in diameter) were used in a sealed cylindrical stainless steel vial, under argon atmosphere. The weight ratio of ball-to-powder was 30 : 1. Secondly, the raw powders were mixed in polyethylene bottles, using zirconia balls with ethanol, and then the weight ratio of ball-to-powder was 10 : 1. This was performed at a horizontal rotation velocity of 250 rpm for 10 h.

After milling, the milled powders were placed in a WC die (outside diameter, 40 mm; inside diameter, 5 mm; height, 40 mm) and then introduced into the pulsed current activated sintering system made by Eltek in South Korea, which is shown schematically in Fig. 2. The four major stages in the sintering are as follows. The system was evacuated (stage 1), and a uniaxial pressure of 1 GPa was applied (stage 2). A pulsed current (on time: 20 μs; off time: 10 μs) was then activated, and maintained to 700 °C with heating rate of 200 °C/min, and then turned off, without holding time (stage 3). The temperatures were measured, using a pyrometer focused on the surface of the WC die. At the end of the process, the sample was cooled to room temperature (stage 4). The process was carried out under a vacuum of 5.33 Pa.

The grain size of ZrO_2 was calculated by Suryanarayana and Grant Norton's formula [12]:

$$B_r(B_{crystalline}+B_{strain})\cos\theta = k\lambda/L + \eta\sin\theta \quad (1)$$

where, B_r is the full width at half-maximum (FWHM) of the diffraction peak, after instrumental correction; $B_{crystalline}$ and B_{strain} are the FWHM caused by small grain size and internal stress, respectively; k is a constant (with a value of 0.9); λ is the wavelength of X-ray radiation; L and η are the grain size and internal strain, respectively; and θ is the Bragg angle. The parameters B and B_r follow Cauchy's form with the relationship: $B = B_r + B_s$, where B and B_s are the FWHM of the broadened Bragg peaks and the standard sample's Bragg peaks, respectively.

The relative densities of the sintered sample were measured by Archimedes' method. Microstructural information was obtained from the 2Ti-ZrO_2 composite, which was polished. Compositional and micro structural

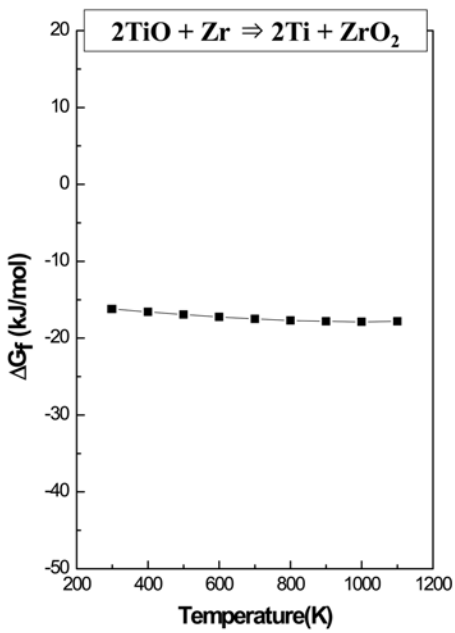

Fig. 3. Temperature dependence of the Gibbs free energy variation by interaction of 2TiO with 2 Zr.

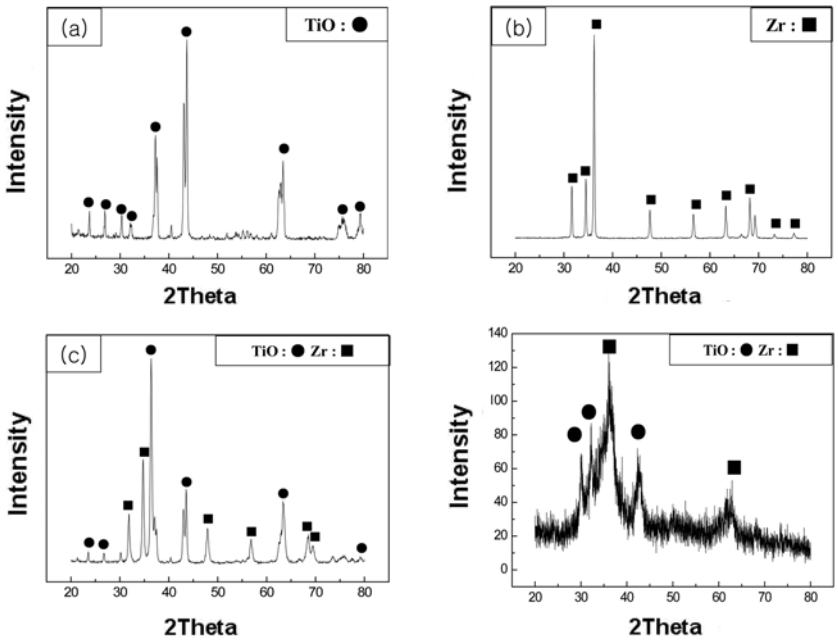

Fig. 4. XRD patterns of raw materials: (a) TiO, (b) Zr , (c) horizontal milled powders and (d) mechanically milled powders.

analyses of the products were made through X-ray diffraction (XRD), transmission electron microscope (TEM) and scanning electron microscopy (SEM) with energy dispersive X-ray analysis (EDAX). Vickers hardness was measured, by performing indentations at a load of 10 kg and a dwell time of 15 s, on the sintered samples.

The wear resistance test using pin-on-disc type apparatus was conducted without a lubricant, with sliding speed of 0.22 m/s and applied load of 100 N. The material of the pin was SKD61, of which the HRC was about 65. The pin was located on a point of radius of gyration, and was kept at 90 degree. We also weighted the pin and the disc, both before and after the test.

A cytotoxicity test was conducted using the fibroblast cell. The fibroblasts were proliferated in Dulbecco's Modified Eagle's Medium (DMEM) with 10% fetal bovine serum (FBS) at 37 ± 1 °C, and the concentration of CO_2 was 5 ± 0.5%. After enough growth, the fibroblasts were seeded at a density of 7×10^3 cells per well, into 96well cell culture plates. They were cultured for 1, 3, and 7days, respectively, with 100 μl of media ionized from the 2Ti-ZrO_2 composite. The cells were treated using CCK-8 solution for 24 h. The absorbance of 2Ti-ZrO_2 composite was measured, using a microplate reader, at 570 nm.

Results and Discussion

The interaction between 2TiO and Zr, i.e.

$$2\ TiO + Zr \rightarrow 2\ Ti + ZrO_2 \qquad (2)$$

is thermodynamically feasible, as shown in Fig. 3.

The X-ray diffraction patterns of horizontal milled powder and mechanically high energy ball milled powders from raw powders are shown in Figs. 4(c) and (d), respectively. The peaks of TiO and Zr were analyzed in the XRD patterns of the horizontal ball milled powders and high energy ball milled powders. The powders milled from the high energy ball milling method or the horizontal ball milling method were not synthesized, but were fined through milling processes. The full width at half-maximum (FWHM) of the diffraction peak is broad, due to the refinement of powder and strain. In this regard, it was considered that powder milled from the high energy ball milling method was smaller, than those from the horizontal ball milling method.

Fig. 5 shows XRD patterns of the high-energy ball milled powder and the horizontal ball milled powder heated to 700 °C, in which only Ti and ZrO_2 peaks are detected. Fig. 6 indicates a plot of $B_r\cos\theta$ versus $\sin\theta$, to calculate the grain size of ZrO_2. The structural parameters, i.e. the average grain sizes of ZrO_2 in composite sintered from horizontal milled powder and high energy ball milled powder, are 91 nm and 45 nm, respectively, which were obtained from the X-ray data in Fig. 5 by Suryanarayana and Grant Norton's formula. It is considered that the average grain sizes of ZrO_2 in composite sintered from horizontal milled powder is higher, than those from high energy ball milled powder, because of the size of the milled powder, since the high energy ball milling method generally has higher impact energy, than does the horizontal ball milling method. The relative densities of the 2Ti-ZrO_2 composites were 97% and 100%, respectively. It is considered that the reasons for the high

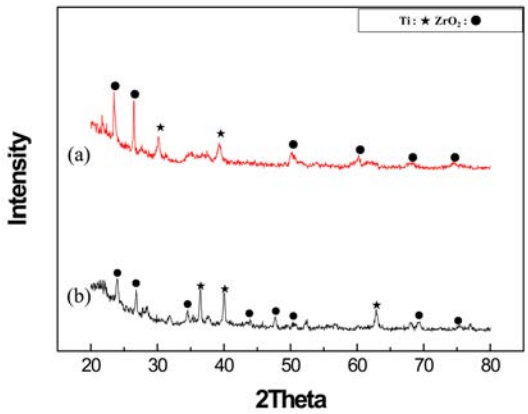

Fig. 5. XRD patterns of 2Ti-ZrO2 composite sintered from (a) high energy ball milled powders and (b) horizontal milled powders.

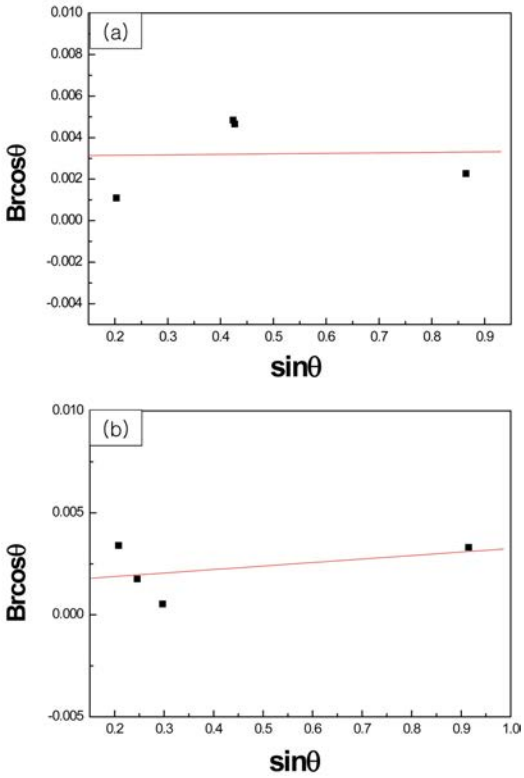

Fig. 6. Plot of Brcosθ versus sinθ of ZrO2 in composite sintered from (a) high energy ball milled powders and (b) horizontal milled powders.

density of the composite obtained at low temperature are as follows. Firstly, the application of pressure during initial stage sintering adds another term to the surface energy driving force, such that the total driving force, F_D, is now [13]

$$F_D = \gamma + (P_a r/\pi), \quad (3)$$

where, γ is the surface energy, Pa is the applied pressure, and r is the radius of the particle.

The effect of pressure on the densification of TiO_2 during high-frequency induction heated sintering was investigated by Shon *et al*. [14]. A significant increase in the relative density was observed, as the pressure was increased from about 60 to 100 MPa, for sintering at 800 °C. Secondly, the role of the current (resistive or inductive) in sintering and or synthesis has been the focus of several attempts aimed at providing an explanation of the observed enhancement of sintering, and the improved characteristics of the products. The role played by the current has been variously interpreted, the effect being explained in terms of the fast heating rate due to Joule heating, the presence of plasma in pores separating powder particles, and the intrinsic contribution of the current to mass transport [15-18].

Fig. 7 shows the SEM image of sample heated to 700 °C, and X-ray mappings. Fig. 7(a) has several differences, compared with Fig. 7(b), in that Ti, O, and Zr elements of the X-ray mappings results are well distributed in Fig. 7(a), and Ti and ZrO_2 phases are not separated very well in Fig. 7(a). Therefore, we were sure that numerous fine Ti and ZrO_2 phases existed in the composite sintered from the high energy ball milled

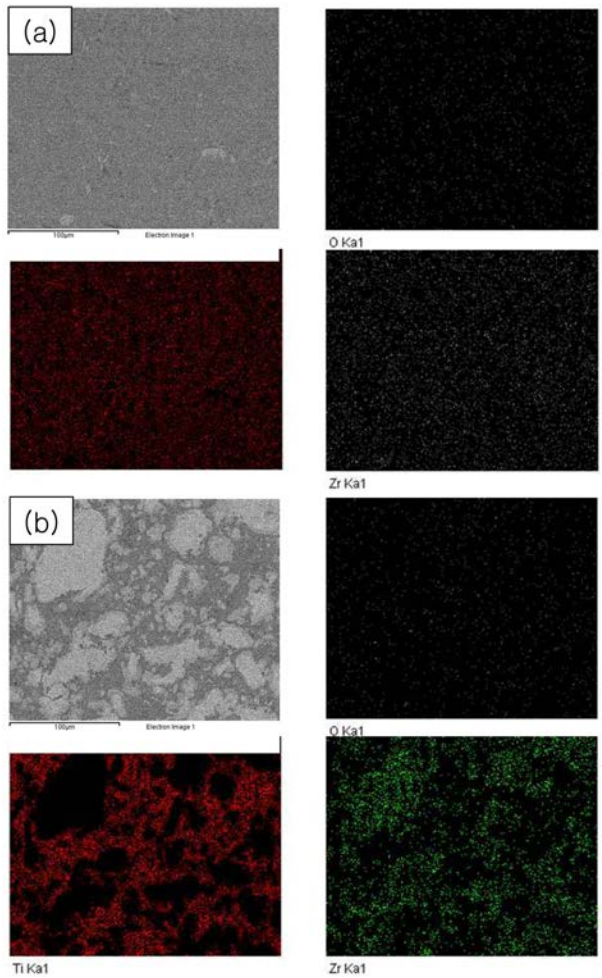

Fig. 7. Scanning electron microscope image and X-ray mapping of 2Ti-ZrO2 system: (a) high energy ball milled powders and (b) horizontal milled powders.

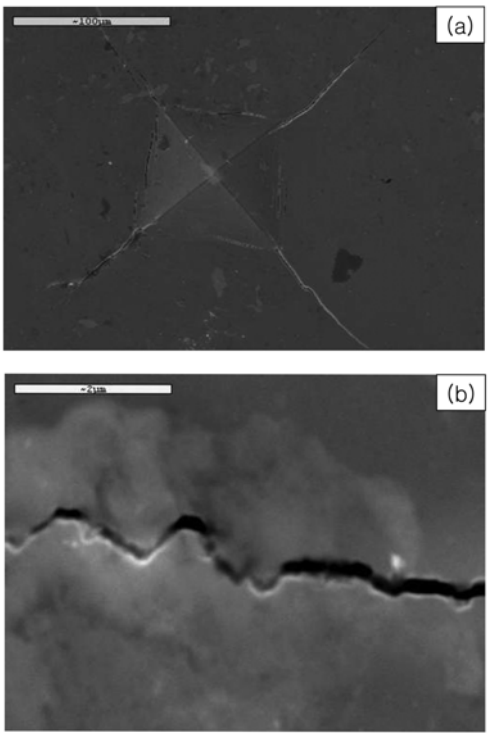

Fig. 8. (a) Vickers hardness indentation and (b) median crack propagating in the 2Ti-ZrO2 composite sintered from high energy ball milled powders.

powder. Fig. 8 shows a high-resolution TEM image of the 2Ti-ZrO_2 composite. The TEM image reveals that atoms are arrayed coherently at the interface of grains. Therefore, it is considered that Ti and ZrO_2 are well bonded. We can also find that the microstructure consists of nanograins.

Vickers hardness measurements were made on polished sections of the 2Ti-ZrO_2 composite, using a 10 kg_f load and 15 s dwell time. The calculated hardness value of 2Ti-ZrO_2 composite sintered at 700 °C from horizontal milled powders and high energy ball milled powders were 990 and 1230 kg/mm^2, respectively. This value represents an average of five measurements. Indentations with large enough loads produced median cracks around the indent. The length of these cracks permits an estimation of the fracture toughness of the material. From the length of these cracks, the fracture toughness values can be determined, using the method of Anstis *et al*. [19], as

$$K_{IC} = 0.016\ (E/H)^{1/2} \cdot P/C^{3/2} \quad (4)$$

where, E is Young's modulus, H the indentation hardness, P the indentation load, and C the trace length of the crack measured from the center of the indentation. The modulus was estimated by the rule of mixtures, for the 0.51 volume fraction of ZrO_2 and the 0.49 volume fraction of Ti, using $E(ZrO_2) = 207$ GPa [5] and $E(Ti) = 116$ Gpa [4]. As in the case of the hardness values, the toughness values were derived

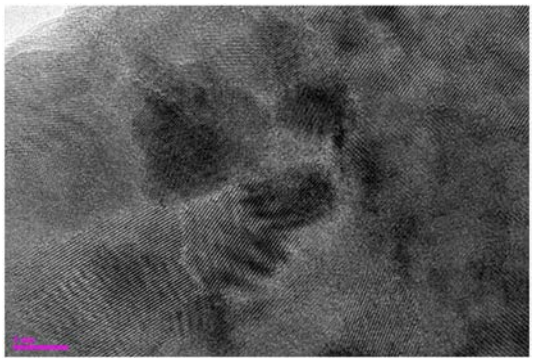

Fig. 9. TEM image of 2Ti-ZrO2 composite heated to 700 °C.

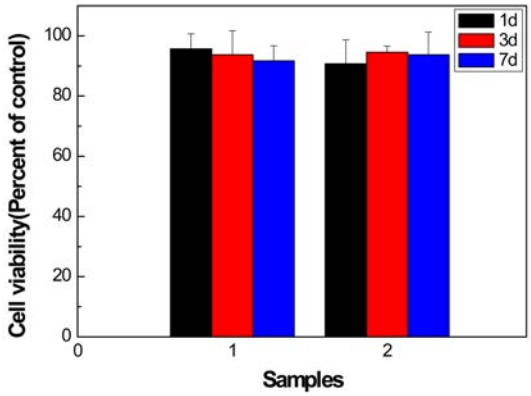

Fig. 10. Measurement of cell viability in Ti(1) and 2Ti-ZrO2 composite using CCK-8 solution on 1, 3, and 7days.

from the average of five measurements. The toughness values of composites obtained from horizontal milled and high energy ball milled powders are 6.5 and 6.8 MPa · $m^{1/2}$, respectively.

The fracture toughness of pure ZrO_2 is reported as 3.3 MPa · $m^{1/2}$ [20]. The fracture toughness of 2Ti-ZrO_2 composite had twice as high value as that of the pure ZrO_2, due to the addition of ductile Ti. Fig. 9(a) shows Vickers indentation in the 2Ti-ZrO_2 composite sintered from high energy ball milled powders. One to three additional cracks were observed to propagate from the indentation corner. A crack propagated in a deflective manner in Fig. 9(b).

Fig. 10 shows the cytotoxicity test of 2Ti-ZrO_2 composite, which is measured by the CCK-8 assay. The CCK-8 assay is one of the most convenient methods that use highly water-soluble tetrazolium salt. By adding tetrazolium to media, we can quantify cell viability, as tetrazolium would change specific color, reacted by the dehydrogenase of mitochondria. The value of the cell viability regarding the 2Ti-ZrO_2 composite was of similar value compared to that of Ti, which is widely known to be used for *in vivo* materials.

Conclusions

TiO and Zr powders were milled by both horizontal ball milling method and high energy ball milling

method. The densification of nano-structured 2Ti-ZrO_2 composites using the pulsed current activated sintering method were sintered from both milled powders within a duration of 4 minutes, and the relative densities of the sintered specimens were 97% and 100%, respectively. The average grain size of ZrO_2 in the composite fabricated from high energy ball milled powder was lower than 100 nm. The average hardness and fracture toughness values obtained from the horizontal ball milled powder and high energy ball milled powder were 990 and 1230 kg/mm^2, and 6.5 and 6.8 MPa · m$^{1/2}$, respectively. The fracture toughness of the 2Ti-ZrO_2 composite is higher than that of pure ZrO_2. The weight loss measured using the type of pin-on-disc apparatus was 8.9×10^{-9} g/m. Lastly, the cell viability portion was higher than 95%, which means that the 2Ti-ZrO_2 composite has almost no toxicity. In conclusion, the 2Ti-ZrO_2 composite showed good mechanical properties (hardness, fracture toughness and wear resistance) and good biocompatibility, and can be used in a hip joint.

Acknowledgments

This research was supported by Basic Science Research Program through the National Research Foundation of Korea (NRF) funded by the Ministry of Education (2012R1A1A4A01001300) and follows the results of a study of the "Leaders Industry-university Cooperation" Project, supported by the Ministry of Education, Science & Technology (MEST).

References

1. N. R. Mohamed and Y. Aihua, Journal of the American Ceramic Society 90 (2007) 1965-1988.
2. B. Bal Sonny, G. Jonathan, R. Michael, and N. R. Mohamed, Seminars in Arthroplasty 17 (2006) 97-101.
3. H. McKellop, F. W. Shen, B. Lu, P. Campbell, and R. Salovey, J. Orthop. Res., 17 (1999) 157-167.
4. S.-M. Chae, J.-S. Park, W. Kim, S.-T. Oh, J.-K. Yoon, and I.-J. Shon, Metal and Materials International 15 (2009) 931-936.
5. K. Morita, K. Hiraga, B.-N. Kim, H. Yoshida, Y. Sakka, Scripta Materialia 53 (2005) 1007-1012.
6. N. R. Kim, S. W. Cho, W. Kim, I. J. Shon, Korean J. Met. Mater. 50, (2012) 34-38.
7. A.I.Y. Tok, L.H. Luo, and F.Y.C. Boey, Materials Science and Engineering: A 383 (2004) 229-234.
8. Geon-Woo Lee, In-Jin Shon, Korean J. Met. Mater. 51, (2013) 95-100.
9. S.-M. Kwak, H.-K. Park, J.-M. Doh, J.-K. Yoon, S.-J. Lee and I.-J. Shon, Journal of Ceramic Processing Research 14 (2013) 65-69.
10. I.J. Shon, H.Y. Song, S.W. Cho, W.B. Kim, and C.Y. Suh, Korean J. Met. Mater. 50 (2012) 39-44.
11. S. M. Kwak, H. K. Park, I. J. Shon, Korean J. Met. Mater. 51, (2013) 314-348.
12. C. Suryanarayana, and M. Grant Norton, X-ray Diffraction A Practical Approach, Plenum Press, New York, (1998).
13. R.L. Coble, J. Appl. Phys. 41 (1970) 4798-4807.
14. H.-C. Kim, H.-K. Park, I.-J. Shon, I.-Y. Ko, Journal of Ceramic Processing Research 7 (2006) 327-331.
15. Z. Shen, M. Johnsson, Z. Zhao and M. Nygren, Spark Plasma Sintering of Alumina, J. Am. Ceram. Soc. 85 (2002) 1921-1927.
16. J.E. Garay, U. Anselmi-Tamburini, Z.A. Munir, S.C. Glade and P. Asoka-Kumar, Appl. Phys. Lett. 85 (2004) 573-597.
17. J.R. Friedman, J.E. Garay. U. Intermetallics 12 (2004) 589-597.
18. J.E. Garay, J.E. Garay. U. Anselmi-Tamburini and Z. A. Munir, Acta Mater. 51 (2003) 4487-4495.
19. G.R. Anstis, P. Chantikul, B.R. Lawn, D.B. Marshall, J. Am. Ceram. Soc. 64 (1981) 533-538.
20. I.-J. Shon, S.-M. Kwak, Journal of Ceramic Processing Research, submitted (2012).